

A synthetic low-frequency mammalian oscillator

Marcel Tigges¹, Nicolas Dénervaud¹, David Greber¹, Joerg Stelling^{1,2,*} and Martin Fussenegger^{1,3,*}

¹Department of Biosystems Science and Engineering, ETH Zurich, Mattenstrasse 26, CH-4058 Basel,

²Swiss Institute of Bioinformatics, ETH Zurich, CH-8092 Zurich and ³University of Basel, Mattenstrasse 26, CH-4058 Basel, Switzerland

Received November 18, 2009; Revised February 9, 2010; Accepted February 10, 2010

ABSTRACT

Circadian clocks have long been known to be essential for the maintenance of physiological and behavioral processes in a variety of organisms ranging from plants to humans. Dysfunctions that subvert gene expression of oscillatory circadian-clock components may result in severe pathologies, including tumors and metabolic disorders. While the underlying molecular mechanisms and dynamics of complex gene behavior are not fully understood, synthetic approaches have provided substantial insight into the operation of complex control circuits, including that of oscillatory networks. Using iterative cycles of mathematical model-guided design and experimental analyses, we have developed a novel low-frequency mammalian oscillator. It incorporates intronically encoded siRNA-based silencing of the tetracycline-dependent transactivator to enable the autonomous and robust expression of a fluorescent transgene with periods of 26 h, a circadian clock-like oscillatory behavior. Using fluorescence-based time-lapse microscopy of engineered CHO-K1 cells, we profiled expression dynamics of a destabilized yellow fluorescent protein variant in single cells and real time. The novel oscillator design may enable further insights into the system dynamics of natural periodic processes as well as into siRNA-mediated transcription silencing. It may foster advances in design, analysis and application of complex synthetic systems in future gene therapy initiatives.

INTRODUCTION

The rapidly developing field of synthetic biology has emerged as a discipline capable of linking theoretical

model predictions to experimental implementations consisting of minimal modular building blocks arranged to form synthetic networks (1) with different levels of complexity (2–9). Substantial information on such minimal units and circuitry originated from prokaryotes (10–18) and the relatively recent development of heterologous mammalian gene regulation technologies (19–21) enabled subsequent applications in complex mammalian systems (2,3,22,23).

In synthetic biology, oscillatory behavior has gained substantial attention due to its impact on repair (24), metabolic (25) and signaling pathways (26–27). Such pathways, like the *p53-mdm2*-triggered apoptosis cascade (28), NF- κ B-regulated immune responses (29) or *Hes1*-mediated developmental control (30), are based on periodic induction of negative feedback loops controlling expression of key pathway factors (31,32).

Utilizing antisense-mediated silencing of a transactivator, we have recently created a synthetic gene network capable of oscillatory expression of the green fluorescent protein (22). Future applications, however, are expected to require fine-tuning of oscillatory properties, such as frequency and amplitude. This could be achieved by alternative selection and reconfiguration of the underlying modular building blocks. Here, we present an alternative oscillatory network that displays robust low-frequency fluctuations in target gene expression. Capitalizing on recent progress showing that RNA interference may be a powerful component of synthetic gene networks (33,34), we have designed a synthetic mammalian clock that combines siRNA-mediated, time-delayed negative feedback loop with autoregulated expression of the tetracycline-dependent transactivator (tTA). The experimental data thus obtained were in good agreement with a mathematical model based on ordinary differential equations. Information gained from such combined dynamic studies should facilitate advances in our understanding of natural circadian clocks and rhythms (35).

*To whom correspondence should be addressed. Tel: +41 61 387 31 60; Fax: + 41 61 387 39 88; Email: fussenegger@bsse.ethz.ch
Correspondence may also be addressed to Joerg Stelling. Tel: +41 61 387 31 94; Fax: +41 61 387 39 94; Email: joerg.stelling@bsse.ethz.ch
Present address:

Nicolas Dénervaud, Institute of Bioengineering, EPFL, Station 17, CH-1015 Lausanne, Switzerland.

MATERIALS AND METHODS

Expression vector design

pBP283 ($P_{ETR3} \rightarrow d2EYFP$), harboring a destabilized enhanced yellow fluorescent protein (d2EYFP) under control of the erythromycin-responsive promoter (P_{ETR3}), was constructed by excising d2EYFP from pd2EYFP (Clontech) using EcoRI/NotI and cloning it into the corresponding sites (EcoRI/NotI) of pBP90 (36). pDG156 ($P_{hCMV^{*-1}} \rightarrow ET1$), containing the erythromycin-dependent transactivator [ET1, E-VP16; (37)] driven by the tetracycline-responsive promoter ($P_{hCMV^{*-1}}$) was designed by excising $P_{hCMV^{*-1}}$ from pMF111 (38) by SspI/EcoRI and cloning it into the corresponding sites (SspI/EcoRI) of pWW35 (19). pDG157 ($P_{hCMV^{*-1}} \rightarrow E\text{-}siRNA_{LUC}\text{-VP16}$) expresses the ET1, E-VP16; (37) containing an intronically encoded siRNA specific for firefly luciferase mRNAs ($siRNA_{LUC}$; nt 62–80). pDG157 was obtained by replacing P_{SV40} of pDG17 (39) with $P_{hCMV^{*-1}}$ (40) via SspI/EcoRI. pDG178 ($P_{hCMV^{*-1}} \rightarrow tTA$) harboring an autoregulated expression unit for tetracycline-responsive control of the tTA was obtained by excising tTA from pSAM200 (38) using EcoRI/BssHIII into pDG156, thereby replacing ET1. pND10 ($P_{hCMV^{*-1}} \rightarrow TAG_{LUC}\text{-}tTA$) contains an expression unit for $P_{hCMV^{*-1}}$ -driven expression of the tTA preceded by a noncoding sequence tag derived from the firefly luciferase coding sequence (nt 62–80). pND10 was constructed in two steps, first by replacing $P_{hCMV^{*-1}}$ of pDG178 with $P_{hEF1\alpha}\text{-}TAG_{LUC}$ ($P_{hEF1\alpha}$, human elongation factor 1 α promoter) of pDG54 via SspI/EcoRI and then by replacing $P_{hEF1\alpha}$ with $P_{hCMV^{*-1}}$ of pDG178 via SspI/KpnI.

Cell culture, transfection and gene regulation

Chinese hamster ovary cells (CHO-K1, ATCC CCL61) were cultivated in ChoMaster[®] HTS (Cell Culture Technologies, Gravesano, Switzerland) supplemented with 5% fetal calf serum (Pan Biotech GmbH, Aidenbach, Germany; cat. no. 3302-P231902, lot no. P231902). CHO-K1 were cultivated at 37°C in a humidified atmosphere containing 5% CO₂, and 35 000 cells were transfected using the FuGENE[®]6 transfection reagent (Roche Molecular Biochemicals, lot. no. 93535720) and a network-encoding plasmid mixture calibrated to a total of 1.2 μ g DNA using the extender vector pcDNA3.1 (Invitrogen, Carlsbad, CA, USA). Transfection experiments were standardized to provide efficiencies of up to 35 \pm 5%. The number of oscillating cells was indicated as percent relative to the total number of transfected cells (100%). Transfected cells were arrested in the G1 phase by a down-shift of the cultivation temperature to 32°C (41), and monitoring of the fluorescence dynamics by time-lapse microscopy was started 18 h posttransfection ($t = 0$).

Fluorescence imaging

Time-lapse fluorescence microscopy was performed using an inverted Leica fluorescence microscope (Leica Microsystems DMI 6000B, 11888107) equipped with an

incubation chamber, a Leica DFC350FX R2 digital camera (Leica, cat. no: 112730043), an 10 \times objective (Leica, Obj. HC PL FL 10 \times /0.30 PH1 -/D 11.0, cat. no. 11506507) and the following excitation/emission filter set: d2EYFP (513/527 nm; C/Y/R, cat. no. 11513897). Time-lapse movies were produced with the LAS AF imaging software (Leica FW4000-TZ, cat. no. 12723979) set to exposure times of 610 ms every 20 min. Fluorescence was quantified for single cells using a custom-designed software implemented in MATLAB[®] (Mathworks, Nantucket/MA, USA) All details on software development are available as Supplementary Data.

Computational modeling

All details on mathematical models and computational methods are provided as Supplementary Data. Simulations were performed with MATLAB[®], Version R2007b.

RESULTS

Design of the low-frequency mammalian oscillator

The low-frequency mammalian oscillator (Figure 1a) consists of: (i) an autoregulated expression unit harboring the tTA and an untranslated *Photinus pyralis* firefly luciferase-derived sequence tag (TAG_{LUC} ; 42, 43) targeted by a luciferase-specific siRNA ($siRNA_{LUC}$; 42) under control of the tTA-specific tetracycline-responsive promoter ($P_{hCMV^{*-1}}$; $P_{hCMV^{*-1}} \rightarrow TAG_{LUC}\text{-}tTA$); (ii) a $P_{hCMV^{*-1}}$ -driven erythromycin-dependent transactivator [ET1; E-VP16; (37)] harboring an intronic $siRNA_{LUC}$ specific for LUC-tagged tTA ($TAG_{LUC}\text{-}tTA$) between the macrolide-dependent repressor (E) and the *Herpes simplex*-derived transactivation domain (VP16) ($P_{hCMV^{*-1}} \rightarrow E\text{-}siRNA_{LUC}\text{-}VP16$); and (iii) a destabilized yellow fluorescent protein variant with a half-life of 2 h (d2EYFP) (44, 45) controlled by the ET1-specific macrolide-responsive promoter (P_{ETR3} ; $P_{ETR3}\text{-}d2EYFP$) (Figure 1a).

When co-transfected into mammalian cells, leaky $P_{hCMV^{*-1}}$ -mediated $TAG_{LUC}\text{-}tTA$ transcription is expected to initiate an autoregulated positive feedback loop sustaining high-level expression of tTA and consequently of $P_{hCMV^{*-1}}$ -driven E- $siRNA_{LUC}\text{-}VP16$ expression. Constitutive splicing of E- $siRNA_{LUC}\text{-}VP16$ produces equimolar amounts of ET1 (E-VP16) and $siRNA_{LUC}$, which results in concomitantly increasing ET1-triggered P_{ETR3} -driven d2EYFP expression and $siRNA_{LUC}$ -mediated breakdown of LUC-tagged tTA transcripts. $siRNA_{LUC}$ -based depletion of $TAG_{LUC}\text{-}tTA$ transcripts will reduce tTA levels and temporarily shut down the network. This results in low d2EYFP expression and low $siRNA_{LUC}$ production, which eventually allows the circuit to start over again. The gene network can be tuned by the addition of tetracycline and erythromycin to regulate $P_{hCMV^{*-1}}$ and P_{ETR3} promoter activity, respectively.

Model-based analysis of circuit behavior

To evaluate the general capability of the network to generate oscillatory behavior, we developed a mathematical

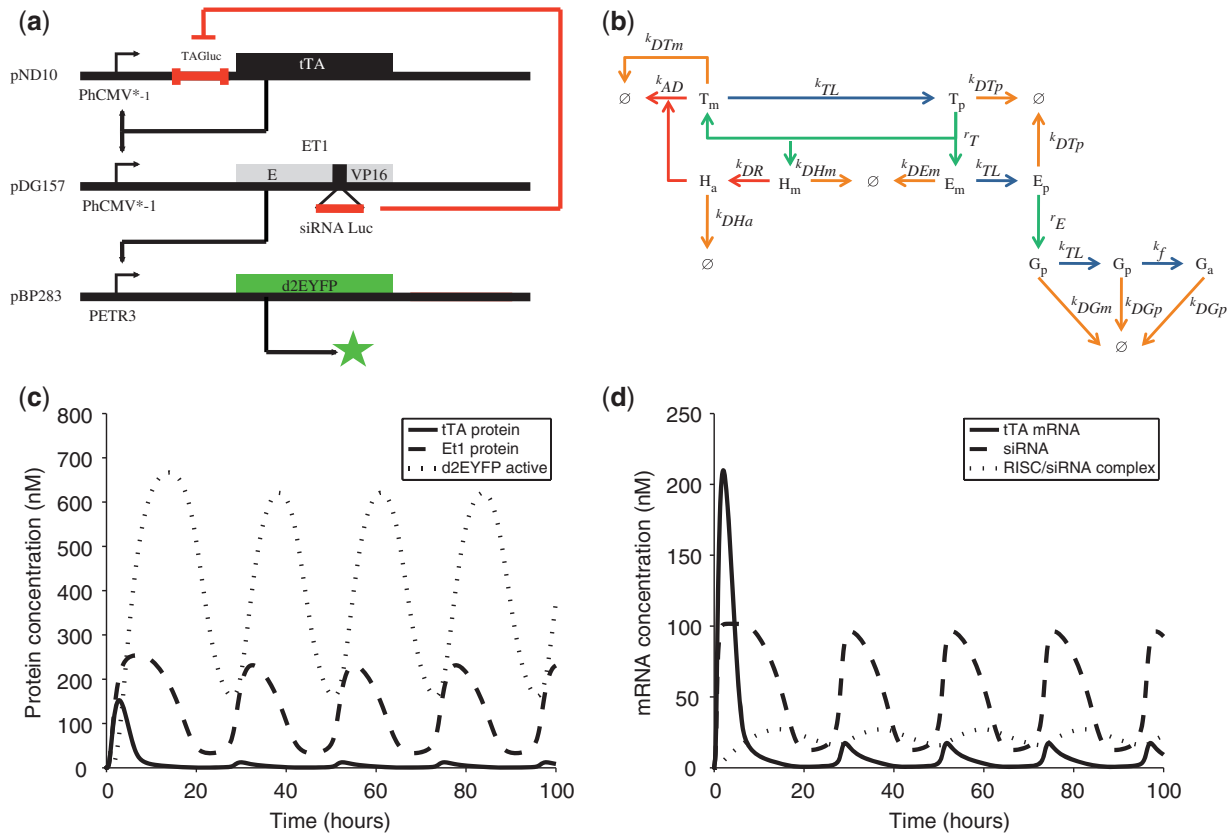


Figure 1. Mammalian clock components and predicted oscillation dynamics. (a) The mammalian oscillator consists of an autoregulated expression unit encoding the tTA under control of the tetracycline-responsive promoter (P_{hCMV^*-1}). A luciferase-specific sequence TAG engineered into the noncoding 5'-region of the tTA transcript enables interference-based silencing of TAG_{LUC}-tTA mRNAs using a luciferase-specific siRNA (siRNA_{LUC}). siRNA_{LUC} is intronically encoded within the macrolide-dependent transactivator (ET1; between the macrolide-responsive repressor (E) and the *Herpes simplex*-derived transactivation domain VP16; E-siRNA_{LUC}-VP16), which is driven by the tTA-specific P_{hCMV^*-1} . Splicing of E-siRNA_{LUC}-VP16 transcripts produces both, siRNA_{LUC}, which triggers interference-based elimination of TAG_{LUC}-tTA mRNAs and ET1, which transactivates P_{ETR3} , thereby controlling expression of the destabilized d2EYFP and enabling visualization of the oscillatory network dynamics. Tetracycline and erythromycin can be used to modulate tTA- and ET1-mediated induction of P_{hCMV^*-1} and P_{ETR3} , respectively. (b) Intracellular processes considered in the mathematical model. Transcription (green arrow), translation and protein folding (blue arrow), degradation (orange arrow) and RNA interference (red arrow). (c and d) Model predictions for the reference parameter set (all plasmids transfected at a 1:1:1 ratio, no antibiotics) (c) with protein concentrations (tTA, solid line; ET1, dashed line; active fluorescent d2EYFP, dotted line) and (d) with mRNA concentrations (tTA, solid line; ET1, dashed line), and RISC/siRNA_{LUC} complex (dotted line).

model based on ordinary differential equations (see Figure 1b and Supplementary Data). This deterministic model describes the circuitry behavior in a mechanistic fashion. A first model prediction based on experimentally determined, as well as literature-based, parameter sets (see Supplementary Data) demonstrated the general capacity of the circuit to display oscillatory gene expression with periods similar to those observed for natural circadian clocks (Figure 1c and d).

Evaluation of circuit behavior in CHO-K1 cells by monitoring d2EYFP expression

According to model simulations, any inactivation of transactivators tTA and/or ET1 by the addition of antibiotics would disrupt the rhythmic expression pattern (Supplementary Figure 1). The impact of regulating antibiotics on the system was therefore first analyzed to validate the functionality of the single components. For this purpose, pND10 ($P_{hCMV^*-1} \rightarrow TAG_{LUC}$ -tTA),

pDG157 ($P_{hCMV^*-1} \rightarrow E$ -siRNA_{LUC}-VP16) and pBP283 ($P_{ETR3} \rightarrow d2EYFP$) were co-transfected at equimolar ratios (1:1:1), followed by subsequent addition of (i) 200 ng/500 μ l tetracycline (Figure 2a) or (ii) 200 ng/500 μ l erythromycin (Figure 2b). As expected, addition of either antibiotic disrupted the oscillatory behavior, leading to decreasing levels of d2EYFP fluorescence overtime.

In contrast, model predictions suggested that the system would be insensitive to variations in the amount of transfected single components (Figure 3 and Supplementary Data). Therefore, we next evaluated the effect of plasmid dosage variations by co-transfecting pND10 ($P_{hCMV^*-1} \rightarrow TAG_{LUC}$ -tTA), pDG157 ($P_{ETR3} \rightarrow E$ -siRNA_{LUC}-VP16) and pBP283 ($P_{ETR3} \rightarrow d2EYFP$) at differing amounts, namely 1:1:1 (100 ng each, Figure 4a), 0.5:0.5:1 (Figure 4b), 2:2:1 (Figure 4c), and varying ratios 2:1:1 (Figure 5a) and 1:2:1 (Figure 5b). All variations displayed oscillatory behavior with similar periods of \sim 26 h and with substantial amplitudes. Hence, the experimental data confirmed the theoretically predicted robustness of

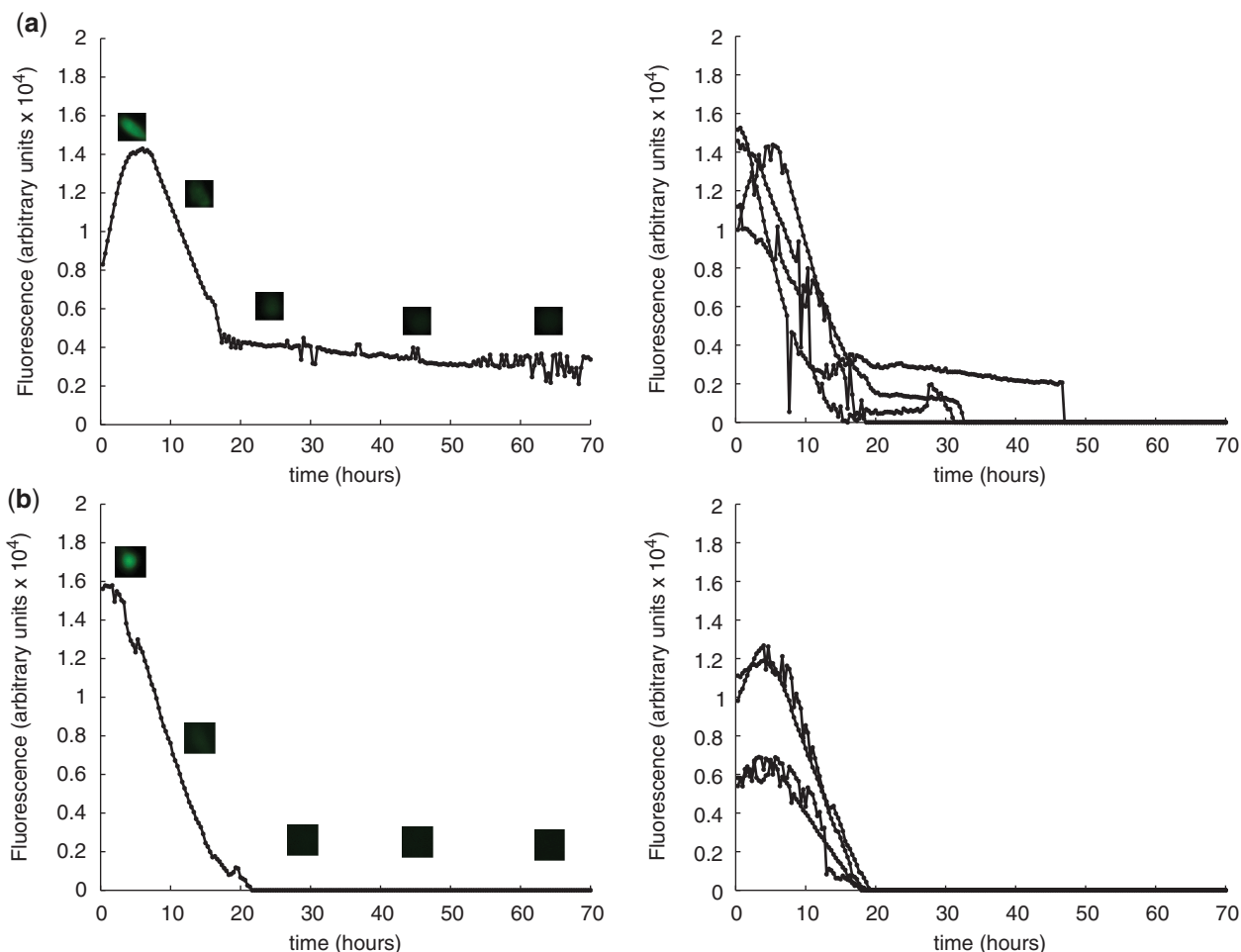


Figure 2. Impact of regulating antibiotics on the mammalian oscillator components and systems behavior using single cell time-lapse fluorescence microscopy of transfected CHO-K1. (a) CHO-K1 co-transfected with pND10 ($P_{hCMV^*-1} \rightarrow TAG_{LUC}$ -tTA), pDG157 ($P_{hCMV^*-1} \rightarrow E$ -siRNA_{LUC}-VP16) and pBP283 ($P_{ETR3} \rightarrow d2EYFP$); 200 ng tetracycline was added to the culture, (b) CHO-K1 transfected with pND10, pDG157 and pBP283; 200 ng erythromycin was added to the culture. Left panels show fluorescence dynamics and micrographs of a representative individual cell, and right panels show the fluorescence profiles of several cells with $t = 0$ corresponding to the onset of fluorescence.

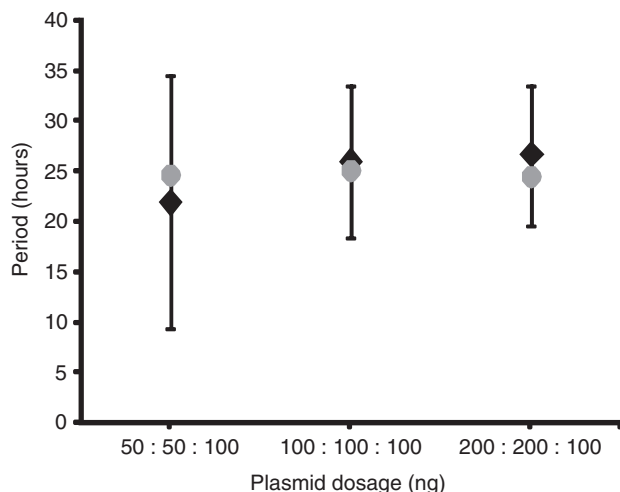


Figure 3. Impact of plasmid dosage on oscillation frequency. Alignment of mathematically simulated and predicted period (gray disc) with the experimental data (black diamonds with error bars) for the conditions (i) pND10 ($P_{hCMV^*-1} \rightarrow TAG_{LUC}$ -tTA);pDG157 ($P_{hCMV^*-1} \rightarrow E$ -siRNA_{LUC}-VP16);pBP283 ($P_{ETR3} \rightarrow d2EYFP$); 50 ng: 50 ng:100 ng, (ii) 100 ng:100 ng:100 ng, (iii) 200 ng:200 ng:100 ng.

the network to moderate changes in the amounts of single components. This contrasts with the observed and predicted sensitivity of the oscillatory behavior to plasmid dosage in our earlier synthetic oscillator based on antisense-mediated silencing of the tTA (22). There, changes in ratio and/or amount of system components influence the period and amplitude of oscillatory gene expression significantly.

When expressing excessive amounts of either pND10 ($P_{hCMV^*-1} \rightarrow TAG_{LUC}$ -tTA) or pDG157 ($P_{ETR3} \rightarrow E$ -siRNA_{LUC}-VP16) using ratios of 10:1:1 (Figure 5c) and 1:10:1 (Figure 5d), the oscillatory circuit was substantially repressed. Interestingly, even with a 10-fold excess in tTA gene dosage, silencing induced visible fluctuations in reporter gene expression (Figure 5c). In contrast, a 10-fold excess of siRNA_{LUC}, which removes TAG_{LUC}-tTA transcripts from the system, completely eliminated such behavior (Figure 5d). These results point to a major role of the amplifying and long-lasting siRNA-mediated silencing mechanism in generating the observed network behavior.

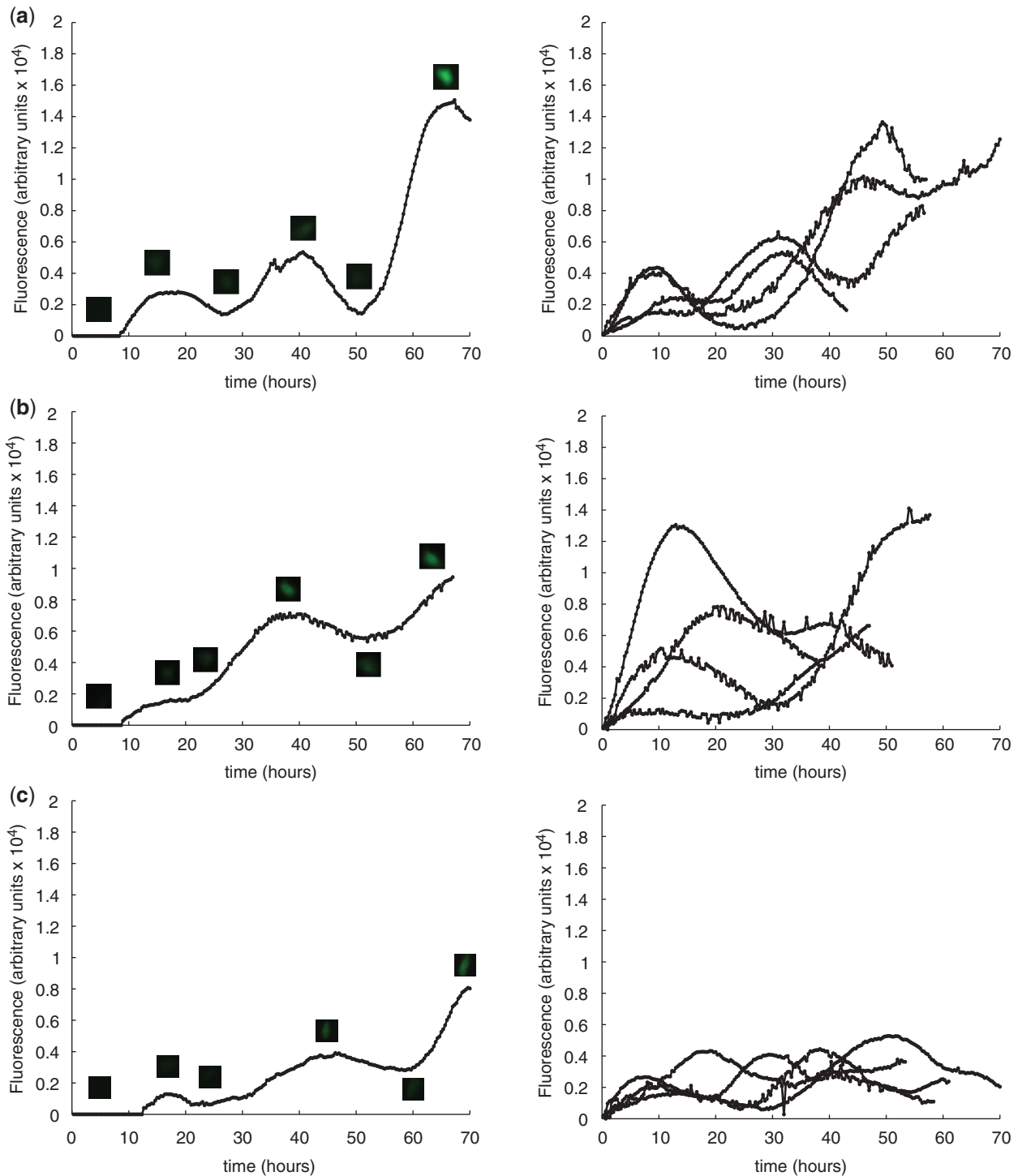


Figure 4. Characterization of oscillator dynamics using single-cell time-lapse fluorescence microscopy of CHO-K1 transfected with different amounts of oscillator components. (a–c) CHO-K1 co-transfected with pND10 ($P_{hCMV^{*1}} \rightarrow TAG_{LUC-tTA}$), pDG157 ($P_{hCMV^{*1}} \rightarrow E-siRNA_{LUC-VP16}$) and pBP283 ($P_{ETR3} \rightarrow d2EYFP$): (a) plasmid ratio of 1:1:1, no antibiotics; (b) 0.5:0.5:1, no antibiotics; and (c) 2:2:1, no antibiotics. Left panels show fluorescence dynamics and micrographs of a representative individual cell, and right panels show the fluorescence profiles of several cells with $t = 0$ corresponding to the onset of fluorescence.

To further characterize the impact of $siRNA_{LUC}$ activity and specificity, we co-transfected CHO-K1 cells with (i) pDG178 ($P_{hCMV^{*1}} \rightarrow tTA$) lacking the 5'- TAG_{LUC} , together with pDG157 ($P_{hCMV^{*1}} \rightarrow E-siRNA_{LUC-VP16}$) and pBP283 ($P_{ETR3} \rightarrow d2EYFP$) and

(ii) pND10 ($P_{hCMV^{*1}} \rightarrow TAG_{LUC-tTA}$), pDG156 ($P_{ETR3} \rightarrow E-VP16$) lacking the intronically encoded $siRNA_{LUC}$ and pBP283 ($P_{ETR3} \rightarrow d2EYFP$) (Figure 6a and b). For both conditions, we detected no oscillations but a constitutive increase in fluorescent intensity

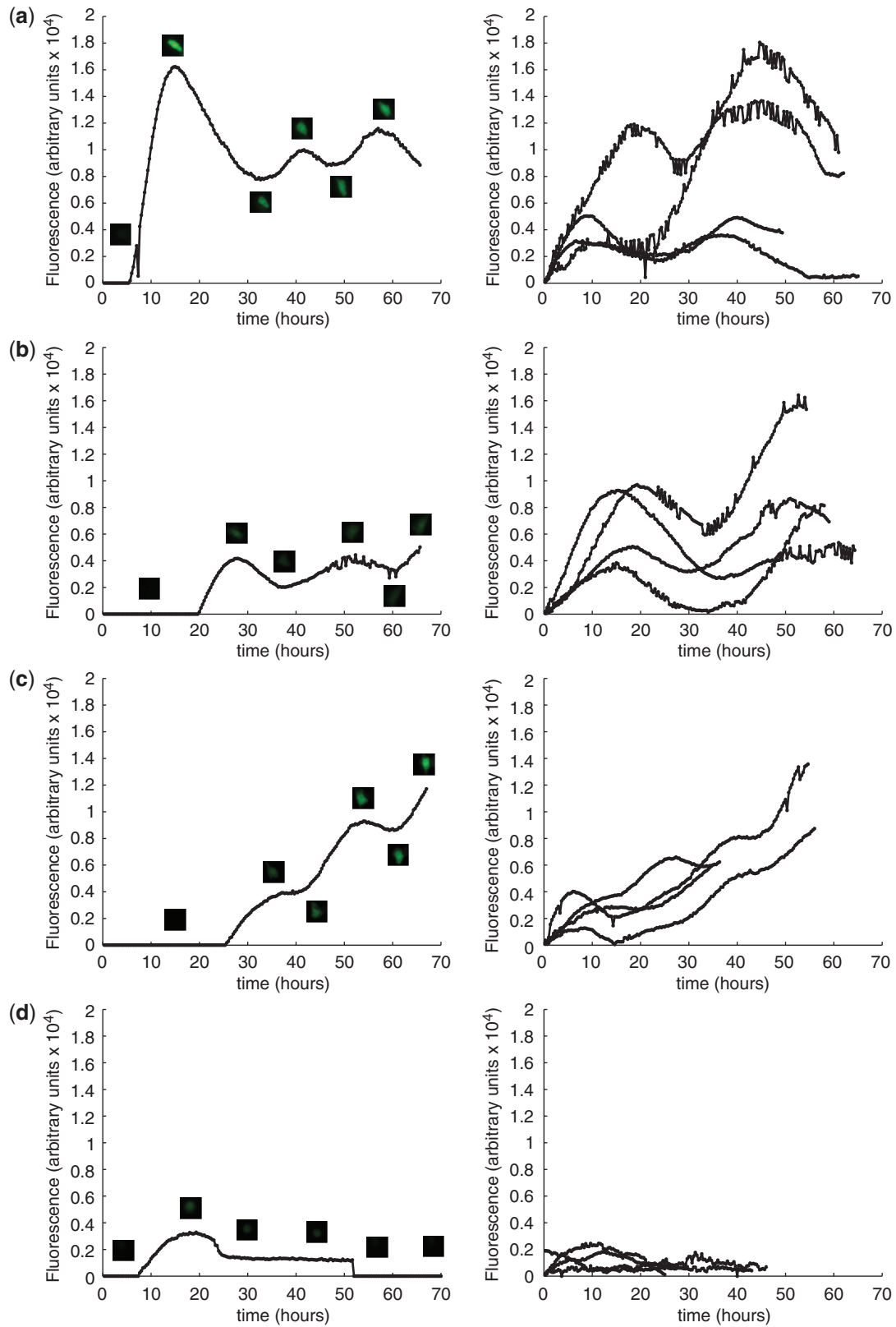


Figure 5. Characterization of oscillator dynamics using single-cell time-lapse fluorescence microscopy of CHO-K1 transfected with different ratios of oscillator components. (a–d) Single-cell time-lapse fluorescence microscopy of CHO-K1 co-transfected with pND10 ($P_{hCMV^*} \rightarrow TAG_{LUC} \rightarrow fTA$), pDG157 ($P_{hCMV^*} \rightarrow E\text{-siRNA}_{LUC} \rightarrow VP16$) and pBP283 ($P_{ETR3} \rightarrow d2EYFP$): (a) plasmid ratio of 2:1:1, no antibiotics; (b) 1:2:1, no antibiotics; (c) 10:1:1, no antibiotics; and (d) 1:10:1, no antibiotics. Left panels show fluorescence dynamics and micrographs of a representative individual cell, and right panels show the fluorescence profiles of several cells with $t = 0$ corresponding to the onset of fluorescence.

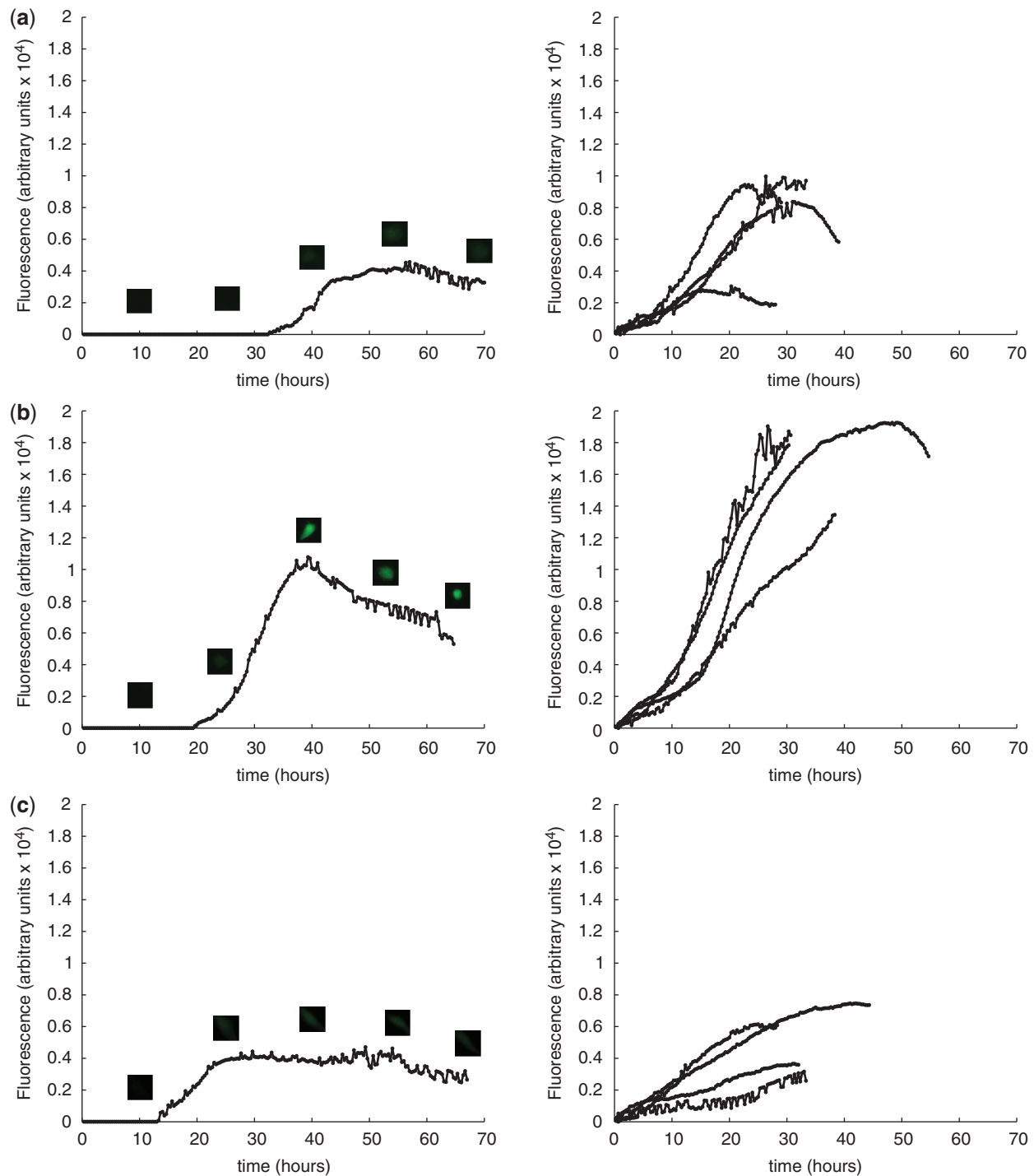


Figure 6. Evaluation of siRNA specificity on the oscillatory behavior using single-cell time-lapse fluorescence microscopy of transfected CHO-K1. (a) CHO-K1 co-transfected with pDG178 ($P_{hCMV^{*}-1} \rightarrow tTA$), pDG157 ($P_{hCMV^{*}-1} \rightarrow E\text{-siRNA}_{LUC}\text{-VP16}$) and pBP283 ($P_{ETR3} \rightarrow d2EYFP$) at a plasmid ratio of 1:1:1, no antibiotics, (b) co-transfection of pND10 ($P_{hCMV^{*}-1} \rightarrow TAG_{LUC}\text{-tTA}$), pDG156 ($P_{hCMV^{*}-1} \rightarrow ET1$; ET1, E-VP16) and pBP283 ($P_{ETR3} \rightarrow d2EYFP$) at a plasmid ratio of 1:1:1, no antibiotics and (c) co-transfection of pDG157 ($P_{hCMV^{*}-1} \rightarrow E\text{-siRNA}_{LUC}\text{-VP16}$) and pBP283 ($P_{ETR3} \rightarrow d2EYFP$) at a plasmid ratio of 1:1, no antibiotics. Left panels show fluorescence dynamics and micrographs of a representative individual cell and right panels show the fluorescence profiles of several cells with $t = 0$ corresponding to the onset of fluorescence.

over time. This was comparable with conditions in which only pDG157 ($P_{hCMV^{*}-1} \rightarrow E\text{-siRNA}_{LUC}\text{-VP16}$) and pBP283 ($P_{ETR3} \rightarrow d2EYFP$) were co-transfected (Figure 6c). The observed oscillatory behavior is therefore specific and directly linked to the $siRNA_{LUC}$ -mediated

elimination of $TAG_{LUC}\text{-tTA}$ transcripts that leads to silencing of tTA expression. These observations confirm functional siRNA-mediated breakdown of target mRNAs and corroborate modeling results based on a specific set of known RNA-interference parameters (see Supplementary

Table 1. Overview on oscillation characteristics resulting from different conditions

Transfected plasmid	Amount (ng)	Antibiotic	No. of cells analyzed	Oscillating cells (%)	Period (h)	Relative amplitude (%)	Figure
pND10:pDG157:pBP283	100:100:100	Tetracycline	109	0 (0.0)	—	—	2a
pND10:pDG157:pBP283	100:100:100	Erythromycin	23	0 (0.0)	—	—	2b
pND10:pDG157:pBP283	100:100:100	None	336	39 (11.6)	25.8 ± 7.6	34.8 ± 22.5	4a
pND10:pDG157:pBP283	50:50:100	None	34	6 (17.6)	23.1 ± 11.5	28.3 ± 17.5	4b
pND10:pDG157:pBP283	200:200:100	None	588	42 (7.1)	26.7 ± 7.0	41.7 ± 21.4	4c
pND10:pDG157:pBP283	200:100:100	None	318	31 (9.7)	26.0 ± 8.5	29.7 ± 16.6	5a
pND10:pDG157:pBP283	100:200:100	None	425	35 (8.2)	25.3 ± 7.5	33.1 ± 19.1	5b
pND10:pDG157:pBP283	1000:100:100	None	192	9 (4.7)	26.7 ± 10.5	33.3 ± 19.7	5c
pND10:pDG157:pBP283	100:1000:100	None	282	0 (0.0)	-	-	5d
pDG178:pDG157:pBP283 (no TAG _{LUC})	100:100:100	None	93	0 (0.0)	-	-	6a
pND010:pDG156:pBP283 (no siRNA _{LUC})	100:100:100	None	152	0 (0.0)	-	-	6b
pDG157:pBP283 (no tTA)	100:100	None	50	0 (0.0)	-	-	6c

ET1, macrolide-dependent transactivator (E-VP16); pBP283 (P_{ETR3}-d2EYFP), expression vector encoding a d2EYFP under control of the erythromycin-responsive promoter; P_{ETR3}, macrolide-responsive promoter (ETR-P_{hCMVmin}); P_{hCMV}, promoter of the human cytomegalovirus immediate early promoter; P_{hCMVmin}, minimal version of P_{hCMV}; P_{hCMV*-1}, tetracycline-responsive promoter (tet_{O7}-P_{hCMVmin}); pDG156 (P_{hCMV*-1}-ET1), expression vector encoding the erythromycin-dependent transactivator (ET1, E-VP16); pDG157 (P_{hCMV*-1}-E-siRNA_{LUC}-VP16), expression vector encoding ET1 containing an intronically encoded siRNA specific for firefly luciferase mRNA (siRNA_{LUC}; nt 62–80); pDG178 (P_{hCMV*-1}-tTA), autoregulated tTA expression vector; pND10 (P_{hCMV*-1}-TAG_{LUC}-tTA), tTA expression vector containing an siRNA_{LUC}-specific tag (TAG_{LUC}) in the 5' untranslated region derived from the firefly luciferase (nt 62–80); siRNA_{LUC}, firefly luciferase-specific siRNA; TAG_{LUC}, firefly luciferase-specific sequence tag; tTA, tetracycline-dependent transactivator (TetR-VP16); VP16, transactivation domain of *Herpes simplex* virus.

Data). Owing to the strong amplification of the mRNA destruction capacity by RNA interference components such as RISC and DICER (46), even residual siRNA levels were predicted to completely eliminate leaky tTA transcripts and, therefore, prevent tTA production (Figure 5c and d).

Quantitative analysis of network behavior using automated image tracking and quantification

To obtain statistically relevant information on the network dynamics, the experimental data were systematically analyzed using customized tracking and image analysis software. Using high-throughput processing of acquired image series (for detailed information see Supplementary Data), we determined a consistent period for all analyzed plasmid ratio variations. In addition, we obtained significant relative amplitudes of >30% for total cellular fluorescence (Table 1).

With respect to the efficiency of oscillator behavior in the cell population, we found the highest number of cells that showed oscillating d2EYFP fluorescence for transfection with equimolar plasmid ratios (1:1:1). A movie showing the oscillatory behavior of the system after transfection of pND10 (P_{hCMV*-1}→TAG_{LUC}-tTA), pDG157 (P_{ETR3}→E-siRNA_{LUC}-VP16) and pBP283 (P_{ETR3}→d2EYFP) at equimolar ratios 1:1:1 (100 ng each) can be found at http://mf-229-serv.ethz.ch/fussi_download/marcel/suppmov.mov. The share of oscillating cells was 11.7% compared to 9.7% (2:1:1), 8.2% (1:2:1), 7.1% (2:2:1) and 17.6% (0.5:0.5:1) (Table 1). In contrast to the first-generation mammalian oscillator (22), which was tunable by varying plasmid ratio and amount (i.e. it exhibited frequency and amplitude changes in response to variations in these parameters), the alternative

low-frequency mammalian oscillator is largely insensitive to component fluctuations.

DISCUSSION

The design of functional replicas of natural circadian clocks using native circadian clock components has been unsuccessful, suggesting that engineering of oscillatory behavior remains a non-trivial challenge (47). Synthetic biology at this point seems to be a valuable alternative, as several synthetic networks in prokaryotic backgrounds have efficiently produced functional circuits displaying damped (48), self-sustained (11), tunable (49,50) or metabolically (51) controlled oscillations. By incorporating posttranscriptional antisense-based control mechanisms, together with transcriptional regulation, we have previously created self-sustained and tunable oscillatory behavior in mammalian cells (22). However, the understanding and availability of single building blocks for complex network reconstruction is still relatively low. Any successful future initiative for gene therapeutic applications will require a broad spectrum of single components that can be interconnected to generate tunable and predictable oscillatory behavior in terms of frequency and amplitude of target gene expression levels. Our intronic-siRNA-based low frequency and robust oscillator therefore not only provides another tool for oscillatory gene expression. Due to its characteristics (siRNA-based feedback loops, long period, robustness to variations of DNA amounts and ratios), it serves as a valuable addition as well as counterpart to established systems. Besides synchronization of oscillators across a population of cells which was recently achieved in bacteria (17,18), the design of synthetic clocks with increased robustness of oscillatory behavior to variations in relative expression

of network components and intrinsic noise remain major challenges on the way to use rhythmic transgene expression dosing in future therapeutic applications. Based on extensive simulations of novel oscillator architectures using a mathematical model, we have chosen to combine a two-level transcription cascade (autoregulated tTA expression triggers expression of the ET1 transactivator which induces d2EYFP expression) with an intronic siRNA-based negative feedback loop eliminating tTA-encoding transcripts by RNA interference. This network design enabled oscillating d2EYFP expression with a fixed frequency and amplitude that was almost insensitive to changes in plasmid ratio and dosage. Such extensions will make custom-tailored designs of regulatory feedback loops for specific applications possible. Furthermore, new insights into intronic siRNA-mediated silencing impact and dynamics may advance the understanding of naturally occurring silencing-mediated feedback and feed-forward circuits.

SUPPLEMENTARY DATA

Supplementary Data are available at NAR Online.

ACKNOWLEDGEMENTS

We thank Wilfried Weber for critical comments on the article.

FUNDING

Swiss National Science Foundation (31003A0-126022); EC Framework 6 (COBIOS). Funding for open access charge: Swiss Federal Institute of Technology, Zurich (ETH Zurich).

Conflict of interest statement. None declared.

REFERENCES

- Hasty,J., McMillen,D. and Collins,J.J. (2002) Engineered gene circuits. *Nature*, **420**, 224–230.
- Weber,W., Daoud-El Baba,M. and Fussenegger,M. (2007) From the Cover: synthetic ecosystems based on airborne inter- and intrakingdom communication. *Proc. Natl Acad. Sci. USA*, **104**, 10435–10440.
- Kramer,B.P., Viretta,A.U., Daoud-El-Baba,M., Aubel,D., Weber,W. and Fussenegger,M. (2004) An engineered epigenetic transgene switch in mammalian cells. *Nat. Biotechnol.*, **22**, 867–870.
- Hu,Z., Killion,P.J. and Iyer,V.R. (2007) Genetic reconstruction of a functional transcriptional regulatory network. *Nat. Genet.*, **39**, 683–687.
- Gardner,T.S., Cantor,C.R. and Collins,J.J. (2000) Construction of a genetic toggle switch in *Escherichia coli*. *Nature*, **403**, 339–342.
- Guido,N.J., Wang,X., Adalsteinsson,D., McMillen,D., Hasty,J., Cantor,C.R., Elston,T.C. and Collins,J.J. (2006) A bottom-up approach to gene regulation. *Nature*, **439**, 856–860.
- Park,J.H. and Lee,S.Y. (2008) Towards systems metabolic engineering of microorganisms for amino acid production. *Curr. Opin. Biotechnol.*, **19**, 454–460.
- Weber,W., Kramer,B.P. and Fussenegger,M. (2007) A genetic time-delay circuitry in mammalian cells. *Biotechnol. Bioeng.*, **98**, 894–902.
- Voigt,C. (2006) Genetic parts to program bacteria. *Curr. Opin. Biotechnol.*, **17**, 548–557.
- Anderson,J.C., Voigt,C.A. and Arkin,A.P. (2007) Environmental signal integration by a modular AND gate. *Mol. Syst. Biol.*, **3**, 133.
- Elowitz,M.B. and Leibler,S. (2000) A synthetic oscillatory network of transcriptional regulators. *Nature*, **403**, 335–338.
- Isaacs,F.J., Dwyer,D.J. and Collins,J.J. (2006) RNA synthetic biology. *Nat. Biotechnol.*, **24**, 545–554.
- Kim,J., White,K.S. and Winfree,E. (2006) Construction of an in vitro bistable circuit from synthetic transcriptional switches. *Mol. Syst. Biol.*, **2**, 68.
- McMillen,D., Kopell,N., Hasty,J. and Collins,J.J. (2002) Synchronizing genetic relaxation oscillators by intercell signaling. *Proc. Natl Acad. Sci. USA*, **99**, 679–684.
- Rosenfeld,N., Elowitz,M.B. and Alon,U. (2002) Negative autoregulation speeds the response times of transcription networks. *J. Mol. Biol.*, **323**, 785–793.
- Rosenfeld,N., Young,J.W., Alon,U., Swain,P.S. and Elowitz,M.B. (2005) Gene regulation at the single-cell level. *Science*, **307**, 1962–1965.
- Danino,T., Mondragon-Palomino,O., Tsimring,L. and Hasty,J. (2010) A synchronized quorum of genetic clocks. *Nature*, **463**, 326–330.
- Fussenegger,M. (2010) Synthetic biology: synchronized bacterial clocks. *Nature*, **463**, 301–302.
- Weber,W., Kramer,B.P., Fux,C., Keller,B. and Fussenegger,M. (2002) Novel promoter/transactivator configurations for macrolide- and streptogramin-responsive transgene expression in mammalian cells. *J. Gene Med.*, **4**, 676–686.
- Weber,W., Marty,R.R., Keller,B., Rimann,M., Kramer,B.P. and Fussenegger,M. (2002) Versatile macrolide-responsive mammalian expression vectors for multiregulated multigene metabolic engineering. *Biotechnol. Bioeng.*, **80**, 691–705.
- Fussenegger,M., Morris,R.P., Fux,C., Rimann,M., von Stockar,B., Thompson,C.J. and Bailey,J.E. (2000) Streptogramin-based gene regulation systems for mammalian cells. *Nat. Biotechnol.*, **18**, 1203–1208.
- Tigges,M., Marquez-Lago,T.T., Stelling,J. and Fussenegger,M. (2009) A tunable synthetic mammalian oscillator. *Nature*, **457**, 309–312.
- Weber,W., Stelling,J., Rimann,M., Keller,B., Daoud-El Baba,M., Weber,C.C., Aubel,D. and Fussenegger,M. (2007) A synthetic time-delay circuit in mammalian cells and mice. *Proc. Natl Acad. Sci. USA*, **104**, 2643–2648.
- Lahav,G. (2004) The strength of indecisiveness: oscillatory behavior for better cell fate determination. *Sci. STKE*, **264**, pe55.
- Zhang,J., Kaasik,K., Blackburn,M.R. and Lee,C.C. (2006) Constant darkness is a circadian metabolic signal in mammals. *Nature*, **439**, 340–343.
- Covert,M.W., Leung,T.H., Gaston,J.E. and Baltimore,D. (2005) Achieving stability of lipopolysaccharide-induced NF-kappaB activation. *Science*, **309**, 1854–1857.
- Fu,L., Pelicano,H., Liu,J., Huang,P. and Lee,C. (2002) The circadian gene *Period2* plays an important role in tumor suppression and DNA damage response in vivo. *Cell*, **111**, 41–50.
- Lahav,G., Rosenfeld,N., Sigal,A., Geva-Zatorsky,N., Levine,A.J., Elowitz,M.B. and Alon,U. (2004) Dynamics of the p53-Mdm2 feedback loop in individual cells. *Nat. Genet.*, **36**, 147–150.
- Krishna,S., Jensen,M.H. and Sneppen,K. (2006) Minimal model of spiky oscillations in NF-kappaB signaling. *Proc. Natl Acad. Sci. USA*, **103**, 10840–10845.
- Yoshiura,S., Ohtsuka,T., Takenaka,Y., Nagahara,H., Yoshikawa,K. and Kageyama,R. (2007) Ultradian oscillations of *Stat*, *Smad*, and *Hes1* expression in response to serum. *Proc. Natl Acad. Sci. USA*, **104**, 11292–11297.
- Jensen,M.H., Sneppen,K. and Tiana,G. (2003) Sustained oscillations and time delays in gene expression of protein *Hes1*. *FEBS Lett.*, **541**, 176–177.
- Tiana,G., Krishna,S., Pigolotti,S., Jensen,M.H. and Sneppen,K. (2007) Oscillations and temporal signalling in cells. *Phys. Biol.*, **4**, R1–17.

33. Deans, T.L., Cantor, C.R. and Collins, J.J. (2007) A tunable genetic switch based on RNAi and repressor proteins for regulating gene expression in mammalian cells. *Cell*, **130**, 363–372.
34. Greber, D., El-Baba, M.D. and Fussenegger, M. (2008) Intronicly encoded siRNAs improve dynamic range of mammalian gene regulation systems and toggle switch. *Nucleic Acids Res.*, **36**, e101.
35. Benner, S.A. and Sismour, A.M. (2005) Synthetic biology. *Nat. Rev. Genet.*, **6**, 533–543.
36. Kramer, B.P., Weber, W. and Fussenegger, M. (2003) Artificial regulatory networks and cascades for discrete multilevel transgene control in mammalian cells. *Biotechnol. Bioeng.*, **83**, 810–820.
37. Weber, W., Fux, C., Daoud-el Baba, M., Keller, B., Weber, C.C., Kramer, B.P., Heinzen, C., Aubel, D., Bailey, J.E. and Fussenegger, M. (2002) Macrolide-based transgene control in mammalian cells and mice. *Nat. Biotechnol.*, **20**, 901–907.
38. Fussenegger, M., Moser, S., Mazur, X. and Bailey, J.E. (1997) Autoregulated multicistronic expression vectors provide one-step cloning of regulated product gene expression in mammalian cells. *Biotechnol. Prog.*, **13**, 733–740.
39. Greber, D. and Fussenegger, M. (2007) Mammalian synthetic biology: engineering of sophisticated gene networks. *J. Biotechnol.*, **130**, 329–345.
40. Gossen, M. and Bujard, H. (1992) Tight control of gene expression in mammalian cells by tetracycline-responsive promoters. *Proc. Natl Acad. Sci. USA*, **89**, 5547–5551.
41. Kaufmann, H., Mazur, X., Fussenegger, M. and Bailey, J.E. (1999) Influence of low temperature on productivity, proteome and protein phosphorylation of CHO cells. *Biotechnol. Bioeng.*, **63**, 573–582.
42. Greber, D. and Fussenegger, M. (2007) Multi-gene engineering: simultaneous expression and knockdown of six genes off a single platform. *Biotechnol. Bioeng.*, **96**, 821–834.
43. Xia, H., Mao, Q., Paulson, H.L. and Davidson, B.L. (2002) siRNA-mediated gene silencing in vitro and in vivo. *Nat. Biotechnol.*, **20**, 1006–1010.
44. Li, X., Zhao, X., Fang, Y., Jiang, X., Duong, T., Fan, C., Huang, C.C. and Kain, S.R. (1998) Generation of destabilized green fluorescent protein as a transcription reporter. *J. Biol. Chem.*, **273**, 34970–34975.
45. Prasher, D.C., Eckenrode, V.K., Ward, W.W., Prendergast, F.G. and Cormier, M.J. (1992) Primary structure of the *Aequorea victoria* green-fluorescent protein. *Gene*, **111**, 229–233.
46. Vermeulen, A., Behlen, L., Reynolds, A., Wolfson, A., Marshall, W.S., Karpilow, J. and Khvorova, A. (2005) The contributions of dsRNA structure to Dicer specificity and efficiency. *RNA*, **11**, 674–682.
47. Chilov, D. and Fussenegger, M. (2004) Toward construction of a self-sustained clock-like expression system based on the mammalian circadian clock. *Biotechnol. Bioeng.*, **87**, 234–242.
48. Atkinson, M.R., Savageau, M.A., Myers, J.T. and Ninfa, A.J. (2003) Development of genetic circuitry exhibiting toggle switch or oscillatory behavior in *Escherichia coli*. *Cell*, **113**, 597–607.
49. Stricker, J., Cookson, S., Bennett, M.R., Mather, W.H., Tsimring, L.S. and Hasty, J. (2008) A fast, robust and tunable synthetic gene oscillator. *Nature*, **456**, 516–519.
50. Swinburne, I.A., Miguez, D.G., Landgraf, D. and Silver, P.A. (2008) Intron length increases oscillatory periods of gene expression in animal cells. *Genes Dev.*, **22**, 2342–2346.
51. Fung, E., Wong, W.W., Suen, J.K., Bulter, T., Lee, S.G. and Liao, J.C. (2005) A synthetic gene-metabolic oscillator. *Nature*, **435**, 118–122.